The AAPS Journal (2021) 23: 12
DOI: 10.1208/s12248-020-00548-8

Research Article

Theme: Use of PBPK Modeling to Inform Clinical Decisions: Current Status of Prediction of Drug-Food Interactions
Guest Editor: Filippos Kesisoglou

Understanding Mechanisms of Food Effect and Developing Reliable PBPK Models Using a Middle-out Approach

Xavier J. H. Pepin,[1,8] James E. Huckle,[2] Ravindra V. Alluri,[3] Sumit Basu,[4] Stephanie Dodd,[5] Neil Parrott,[6] and Arian Emami Riedmaier[7]

Received 22 October 2020; accepted 7 December 2020; published online 4 January 2021

Abstract. Over the last 10 years, 40% of approved oral drugs exhibited a significant effect of food on their pharmacokinetics (PK) and currently the only method to characterize the effect of food on drug absorption, which is recognized by the authorities, is to conduct a clinical evaluation. Within the pharmaceutical industry, there is a significant effort to predict the mechanism and clinical relevance of a food effect. Physiologically based pharmacokinetic (PBPK) models combining both drug-specific and physiology-specific data have been used to predict the effect of food on absorption and to reveal the underlying mechanisms. This manuscript provides detailed descriptions of how a middle-out modeling approach, combining bottom-up *in vitro*-based predictions with limited top-down fitting of key model parameters for clinical data, can be successfully used to predict the magnitude and direction of food effect when it is predicted poorly by a bottom-up approach. For nefazodone, a mechanistic clearance for the gut and liver was added, for furosemide, an absorption window was introduced, and for aprepitant, the biorelevant solubility was refined using multiple solubility measurements. In all cases, these adjustments were supported by literature data and showcased a rational approach to assess the factors limiting absorption and exposure.

KEY WORDS: food effect; middle out; modeling; optimization; PBPK; pharmacokinetics.

INTRODUCTION

The consumption of food around drug dosing time can alter absorption of an orally administered medicine (1). Over the last 10 years, 40% of the oral drugs approved by the FDA or EMA show a significant effect of food on their pharmacokinetics (PK) (2). Therefore, determination of the magnitude and direction of food effect is required prior to drug approval by health authorities and the result informs the drug label on dosing recommendation (3, 4). Currently, a clinical food effect study is the only data that is accepted by the health authorities. However, on its own, a clinical study does not provide mechanistic understanding for the food effect (2).

Since many mechanisms can lead to a food effect (5, 6), physiologically based pharmacokinetic (PBPK) models, which combine drug-related properties and physiology-specific data, can be used to uncover the mechanisms underlying the effects of food on oral absorption (7–9). It also helps in minimizing the number of clinical FE studies by simulating the food effect when changes are made to critical quality attributes of formulations during drug development. In an accompanying manuscript, a unique approach was utilized to build and verify mechanistic PBPK models for 30 compounds while controlling for common variables, such as differences in input data, method of data generation, and subjective optimization and/or verification (10). The focus of that work was to identify food effect mechanisms associated with high, moderate, or low prediction confidence. The levels of confidence were defined based on the stage of drug development and an assessment of how the PK parameters and profiles were captured.

Guest Editor: Filippos Kesisoglou

[1] New Modalities and Parenteral Development, Pharmaceutical Technology & Development, Operations, AstraZeneca, Macclesfield, UK.
[2] Drug Product Technology, Amgen, Thousand Oaks, California, USA.
[3] Clinical Pharmacology and Safety Sciences, R&D, AstraZeneca, Cambridge, UK.
[4] Pharmacokinetic, Pharmacodynamic and Drug Metabolism-Quantitative Pharmacology and Pharmacometrics (PPDM-QP2), Merck & Co., Inc., West Point, Pennsylvania, USA.
[5] Chemical & Pharmaceutical Profiling, Novartis Institutes for Biomedical Research, Cambridge, Massachusetts, USA.
[6] Pharmaceutical Sciences, Roche Pharmaceutical Research and Early Development, Roche Innovation Center, Basel, Switzerland.
[7] DMPK and Translational Modeling, AbbVie Inc., North Chicago, Illinois, USA.
[8] To whom correspondence should be addressed. (e–mail: Xavier.pepin@astrazeneca.com)

1550-7416/21/0100-0001/0 © 2021 American Association of Pharmaceutical Scientists

Out of the 30 drugs studied in this work, 8 compounds were classified as a high confidence prediction, following a middle-out simulation approach (11), after the initial bottom-up food effect predictions did not capture the C_{max} and AUC within 2-fold. The current manuscript describes the modeling approaches and outcomes for nefazodone, furosemide, and aprepitant. The middle-out approach integrates information from *in vitro* or *in silico* experiments with information derived from observed clinical studies, using both GastroPlus™ and Simcyp®. For illustration purpose, only results from one software package are presented for each drug. However, additional simulations are performed to illustrate the mechanisms limiting the absorption of the drugs studied here, and how they are captured by both software platforms. In particular, the gastrointestinal (GI) fluid volumes are varied to harmonize them across the two modeling platforms and the impact on simulation results is presented.

MATERIALS AND METHODS

PBPK input parameters in this work such as permeability, solubility, or dissolution were measured by consistent methods. For more detailed description of methods used to generate this data, the reader is directed to Emami Riedmaier *et al.* (10). The surface pH of nefazodone HCl was determined according to Serajuddin *et al.* (12) with minor modifications. Unbuffered solutions were prepared by adjusting a 0.15-M NaCl solution to pH values of 2, 4, and 9 using HCl or NaOH. The pH of each unbuffered solution was determined immediately before starting the experiment. For nefazodone HCl, 3 mL of each solution was added to 500 mg drug substance in an appropriate container, and stirred on a vortex for 10 s, and the pH of the obtained slurry was measured immediately and after 10 min, 1 h, 2 h, and 24 h. The thresholds for definition of "no-food effect" for the drugs of this study are based on the AUC ratio being comprised between 0.8 and 1.25 (10).

Modeling Approach

PBPK models were built for furosemide in Simcyp® V17.1 (Certara, USA, Inc.) and for nefazodone and aprepitant in Simcyp® V18.0 (Certara, USA, Inc.). For nefazodone and furosemide, GastroPlus™ V9.0 (SimulationsPlus) was used while for aprepitant, GastroPlus™ V9.7 (SimulationsPlus) was used. A software comparison was not the aim of this work. The modeling strategy followed in this work is illustrated in Figure S0.1. Model performance was assessed through the calculation of average fold error (AFE) and absolute average fold error (AAFE), from data points of the PK profiles or from predicted and measured PK parameters according to the following equations.

$$\mathrm{AFE} = 10^{\frac{1}{n}\times\sum \mathrm{Log}\left(\frac{\mathrm{predicted_i}}{\mathrm{observed_i}}\right)}$$

$$\mathrm{AAFE} = 10^{\frac{1}{n}\times\sum \left|\mathrm{Log}\left(\frac{\mathrm{predicted_i}}{\mathrm{observed_i}}\right)\right|}$$

The average fold error indicates whether the predicted values underestimate or overestimate the observed values. The absolute average fold error quantifies the absolute error from the true value (13).

Nefazodone HCl

Nefazodone HCl is an antidepressant drug with BCS class 1 characteristics at the clinical dose of 200 mg. Barbhaiya, R. H., *et al.* reported that, while nefazodone HCl is completely absorbed, it is subjected to large first-pass extraction (14). Thus, the drug is reported to have an absolute bioavailability of 15–27% with large inter-subject variability and single-dose pharmacokinetic profiles show supra-proportional increases in exposure with dose (14–17). The main enzyme involved in nefazodone metabolism is CYP3A4 and nefazodone also inhibits that enzyme, leading to a more linear exposure dose relationship after repeated dosing (17). The approved label for Serzone indicates a 20% reduction in exposure with food (18). Dockens *et al.* reported no effect or a slight negative effect of food (19) based on average plasma profiles. However, the same authors report a reduction of 7% for the C_{max} and 22% for the AUC in the presence of food based on average PK parameters.

For nefazodone, the GastroPlus™ model was built using a compartmental distribution model with parameters estimated by fitting PK data from a 10-min intravenous (IV) infusion of 5 mg dose reported for subject 9 in Barbhaiya, R. H., *et al.* (14). Literature data for CYP3A4 metabolism of nefazodone by human liver microsomes were used to estimate model parameters for V_{max} (10 nmol/min/mg protein) and K_m (452 μM) (20). These values were integrated using the GastroPlus™ conversion tool, assuming a microsomal fraction unbound of 2.46% as estimated by Austin's equation (21). The metabolic clearance was verified against intravenous data. Human permeability values were estimated from this work based on *in vitro* Caco-2 data and the gut CYP3A4 V_{max} scaling was adjusted to match the 200 mg subject 9 oral data (14). The model was then verified on its prediction of the non-linearity observed in the fasted state on C_{max} and AUC for oral nefazodone doses ranging from 50 to 500 mg. The prediction of the food effect was then compared with data from Dockens *et al.* (19).

Furosemide

Furosemide is a powerful loop diuretic indicated in resistant edema or hypertension at a dose ranging from 40 to 80 mg daily. The oral bioavailability of furosemide is reported to be between 43 and 65% in healthy subjects, and this drug can be considered BCS class 4 compound (22, 23). Seventy-five percent of the drug is eliminated unchanged by the kidneys (24). IV data and oral fasted state and fed state data for 40 mg furosemide formulations were used to build, validate, and evaluate the model (25). The PK profile observed after administration of a 40-mg IV bolus injection was fitted to a 3-compartment model and determined total systemic clearance for the GastroPlus™ model. In GastroPlus™, the renal clearance was 75% of the total IV clearance and the rest of the clearance was considered to be metabolic (23). The first-pass gut extraction was considered negligible since liver metabolic first-pass extraction was calculated at less than 3%. In GastroPlus™, a stomach transit

time of 2 h was used in the fed state for the solid formulation instead of the default 1 h to reflect the 90 min emptying time reported for solid formulations (26).[1] Conflicting data exist for furosemide's permeability in human. The human jejunal effective permeability was measured at 0.05×10^{-4} cm/s by Lennernäs *et al.* with the Loc-I-Gut system, but in an open perfusion system, furosemide permeability was measured at 0.5×10^{-4} cm/s in the jejunum and 0.2×10^{-4} cm/s in the ileum by the same author (27). In another study, 40 mg furosemide solutions were infused in the duodenum of humans and the human P_{eff} estimate for the duodenum was much higher at 7×10^{-4} cm/s (28), suggesting a narrow absorption window in the upper GI tract. In GastroPlus™, a bottom-up approach was attempted using a constant model human P_{eff} of 0.5×10^{-4} cm/s. However, this was not successful and so, using a middle-out approach, the permeability of the GI tract compartments was adjusted to capture the absorption window and match the oral PK profile observed in the fasted state at 40 mg. The permeability in the duodenum was set to 1.2×10^{-4} cm/s and the 0.5×10^{-4} cm/s measured by Lennernäs was used in the jejunum. For all the subsequent GI compartments, the value of 0.05×10^{-4} cm/s was used. Since this drug is a substrate of P-gp, a more mechanistic approach was also tried using the Tachibana model and is described in the supplementary materials.

Aprepitant

Aprepitant, a selective high-affinity antagonist of human substance P/neurokinin 1 receptors, is the active ingredient of EMEND®, which has been approved by the FDA for the prevention of chemotherapy-induced nausea and vomiting. The early clinical formulation was a tablet with micronized particle size, which showed positive food effect in healthy human volunteers given a high-fat breakfast (2.8-fold increase AUC, 2.2-fold increase in C_{max}) (29). The final marketed composition capsules contain a nanosuspension, which improved oral bioavailability compared to micronized formulations by approximately 2-fold in man in the fasted state. The marketed formulation bioavailability is 67% at 80 mg and 59% at 125 mg. Oral administration of the nanosuspension capsule with a standard high-fat breakfast had no clinically meaningful effect on the bioavailability of aprepitant (fed/fast AUC ratios: 1.09 and 1.2 at 80 mg and 125 mg, respectively) (30). PBPK models for micronized and nanoparticle formulations were built in Simcyp®. Aprepitant is a weak base in the physiological pH range with an acid pK_a of 9.15 and base pK_a of 2.45 (31). The compound is poorly soluble in aqueous media with reported solubility values varying from 0.7 μg/mL in SIF at pH 6.5 to 7.0 μg/mL in water at pH 8.0 (32, 33). The biorelevant solubility and dissolution in biorelevant media for both micronized and nanoparticle formulation were extracted from multiple references (33, 34) and were used to estimate $\log K_{m:w}$ values and diffusion layer model (DLM) scalars using SIVA®[2] or to fit the *Z*-factor model in GastroPlus™ to the dissolution data for micronized formulations (see supplementary material 4). The apparent permeability (P_{app}) values measured by the IQ consortium in MDCK cell lines for aprepitant (13.0×10^{-6} cm/s) were used to calculate a $P_{eff,man}$ of 2.4×10^{-4} cm/s. The P_{app} (15.0×10^{-6} cm/s) of high permeability calibrator propranolol in the same experiment was used to obtain a scalar within Simcyp. The IV PK profile observed after a 4-h infusion of 2 mg stable isotope-labeled aprepitant dosed with 125 mg unlabeled aprepitant administered orally was used to estimate the distribution parameters (V_{sac}, K_{in}, and K_{out}) in Simcyp® (30) and the reported systemic CL was incorporated into the model. Since aprepitant is predominantly metabolized by CYP3A4 (35), the contribution of intestinal first pass was incorporated using the default estimation method in the Simcyp® simulator based on reported total clearance and assuming 100% CYP3A contribution. Then, the oral PK profile of 100 mg micronized aprepitant was simulated in fasted individuals after incorporating physicochemical properties, permeability, and dissolution data described above (34). After verification of successful prediction of the fasted state PO PK profile, the model was used to predict the impact of food on oral absorption.

RESULTS

Nefazodone HCl

The main model input parameters for nefazodone HCl are given in Table I and detailed results on solubility and surface pH are provided in supplementary material 1. The default *in vitro* to *in vivo* scaling for liver CYP3A4 metabolism led to a good bottom-up prediction of the IV profile for both software platforms and no scaling factor adjustment was needed (supplementary material 5). The PK profile simulation for an oral solution dosed to subject 9 is shown in Fig. 1. The PBPK model was verified against ascending dose PK data collected from multiple parallel studies (14, 17, 19). The PK non-linearity observed on day 1 with dose for nefazodone HCl was well predicted with GastroPlus™ even if the model tended to overpredict the measured C_{max} and to a lesser extent the AUC for the higher doses (Fig. 2). The AFE and AAFE for the prediction of AUC over the dose range of 50-500 mg are of 1.04 and 1.09 respectively. The AFE and AAFE for the prediction of C_{max} over the dose range of 50-500 mg are of 1.10 and 1.21 respectively. The prediction of Dockens *et al.* (19) fasted and fed state median pharmacokinetic profiles following 200 mg oral tablet administration is shown in Fig. 3. Since population PK parameters report a 50% relative standard deviation (RSD) in the fed state and 60% RSD in the fasted state, the median PK profiles in both prandial conditions are plotted with standard deviation calculated from these RSD values. Profiles in the fasted state were predicted with single-phase gastric emptying or using a double peak through the multiple mixed dose (MMD) function of GastroPlus™. Indeed, the median ($n = 24$) PK profiles for nefazodone tablet in the fasted state show an apparent double peak and the occurrence of double peaks in the fasted state is in contrast with the single peak observed for the oral 200 mg solution (Fig. 1). There are multiple reasons for the occurrence of double peaks in pharmacokinetics (40). Entero-hepatic circulation was ruled out to explain this secondary peak, since the phenomenon was not observed with the oral solution or IV

[1] In GastroPlus™, the compartment transit time (T) is the inverse of the transit rate constant: T = t1/2Ln2

[2] SIVA® is the Simcyp® *in vitro* (data) analysis toolkit which allows to extract model parameters from *in vitro* data.

Table I. Nefazodone HCl Modeling Input Parameters for Simcyp® and GastroPlus™

Parameter	Simcyp®	GastroPlus™	References/rationale
Molecular weight (g/mol)	470		(36)
Compound nature	Crystalline, HCl salt		
pK_a	6.5 (B)		(37)
Log *P*	Log *P* = 4.7		(38)
True density (g/mL)	1.2		Default
Intrinsic solubility (μg/mL)	Free base (3.98 μg/mL at pH 9), salt = 7.6 mg/mL at pH_{max} = 3.3		Measured in this study for the salt
FaSSIF-V2 solubility (mg/mL)	1.393 at final pH = 6.9		Measured in this study
FeSSIF solubility (mg/mL)	3.1 at final pH = 5.05		Measured in this study
log ($K_{m:w}$)	6.4 for the neutral drug and 0 for the ionized drug	NA	Fitted to FaSSIF and FeSSIF data
Solubilization ratio	NA	2.34E+6	Fitted to FaSSIF and FeSSIF data
Solubility factor	1909	1910.4	Fitted to salt solubility using built-in tools for solubility-pH profiles
F_u plasma (%)	1		(18)
B/P ratio	0.85		Simcyp® prediction
Particle size diameter (μm)	10		
F_u enterocyte (%)	100		
Jejunum P_{eff} (10^-4 cm/s)	2.2		Measured in this study (Caco-2)
Formulation type	200 mg immediate release (solution and tablet)		
Model for dissolution	DLM default	Johnson, effect of BS on solubility and diffusion	
Precipitation	CSR = 10,000 PRC = 0.0001 h^{-1}	T_p = 900 s	No impact of precipitation on exposure
Model for distribution	Model 1 = Poulin (39), K_p scalar = 0.05	2 compartments	Fitted to 5 mg 10 min IV infusion for subject 9 in ref. (14)
Calculated V_{SS} (L/kg)	0.467		
V_c (L/kg), k_{12} (h^{-1}), k_{21} (h^{-1})	NA	0.302, 0.806, 0.59	Fitted to IV data of ref. (14)
IV clearance (L/h/kg)	0.349		Not used but bottom-up approach using K_m and V_{max} for CYP3A4 was introduced in the liver and gut
$F_{u,inc}$ for HLM (%)	2.46		$F_{u,\ calc}$ Austin method in GastroPlus™
V_{max} CYP3A4 (nmol/min/mg protein)	10		(20) Introduced with default options for both software for the liver
K_m CYP3A4 (μM)	452		(20) Introduced with default options for both software for the liver
Gut CYP3A4 SF	NA	0.9	Fitted to 200 mg subject 9 oral solution data in Barbhaiya, R. H., *et al.* (14)

NA not applicable, *DLM* diffusion layer model, *B/P* blood to plasma, F_u fraction unbound, *SF* scaling factor, *FaSSIF* fasted state simulated intestinal fluid, *FeSSIF* fed state simulated intestinal fluid, *CSR* critical supersaturation ratio, *PCR* precipitation rate constant

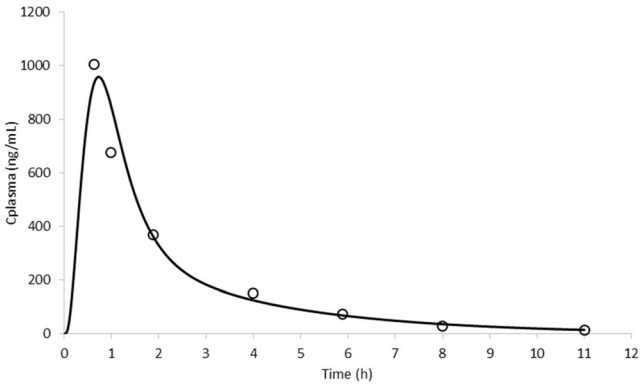

Fig. 1. Prediction of pharmacokinetic profile in fasted state for 200 mg nefazodone solution in patient 9 from Barbhaiya, R. H., *et al.* (14) using GastroPlus™. Symbols show observed data

infusion for this drug, and since subjects were fasted 4 h after dosing (19), while the second peaks occurred around 2 h after dosing. Two hypotheses can be put forward to explain these second peaks: (A) Since both nefazodone-HCl solubility and permeability are high, this drug could be a marker of gastric emptying and partial gastric emptying has been reported for other products in the literature (41, 42). (B) Wettability issues and consequently slow dissolution rates are reported for nefazodone-HCl tablets, despite the high measured equilibrium solubility (43). This poor wettability seems to be a drug substance attribute, as it was also observed in this work during the FaSSIF (but not during FeSSIF) solubility measurements (Figure S1.1). This slow dissolution could be responsible for incomplete release in the stomach and further dissolution in the intestine. To test hypothesis (A), the simulation with partial gastric emptying was done to verify if both C_{max} and AUC could be recovered and what was the impact of double peaks in the first-pass extraction. The MMD released an IR dose of 120 mg at time 0 and 80 mg at 1.3H. The hypothesis (B) was not tested since the authors could not retrieve the dissolution data of the batch used by Dockens *et al.* (19) in their study. However, a slow dissolution in the GI tract would qualitatively lead to a higher first-pass extraction similarly to slower gastric emptying tested in this work.

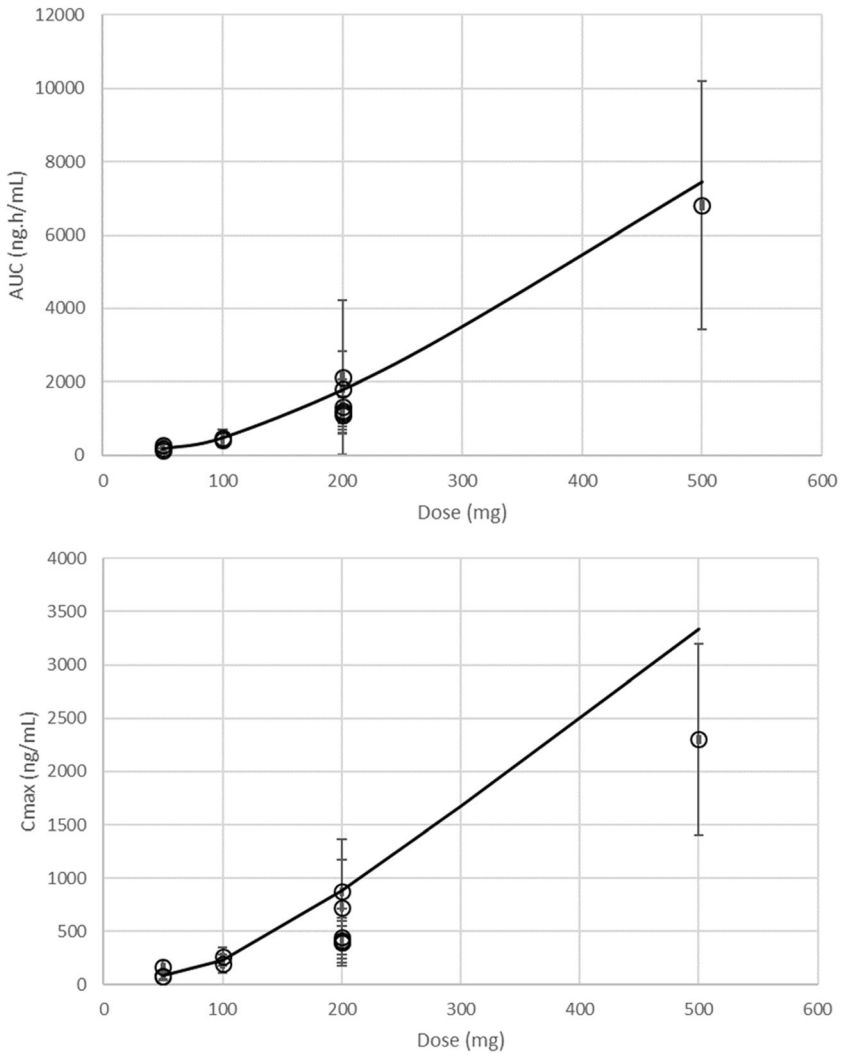

Fig. 2. Prediction of AUC (upper panel) and C_{max} (lower panel) for various doses of nefazodone HCl with GastroPlus™. Measured values from refs (14, 17, 19). Symbols show observed data ± 1SD

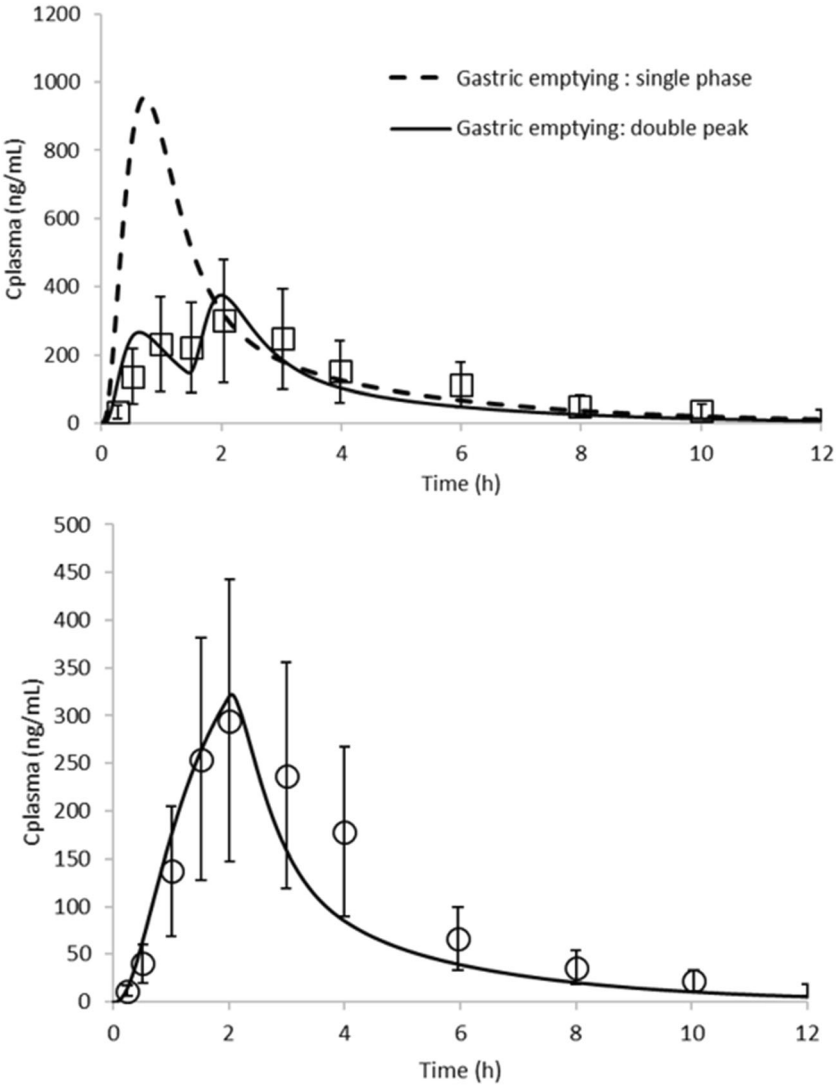

Fig. 3. Prediction of pharmacokinetic profile in fasted (upper panel) and fed (lower panel) states using GastroPlus™ for 200 mg nefazodone-HCl tablets. Data from Dockens *et al.* (19). Symbols show observed data ± 1SD

The simulation of the fasted state with double peak is adequate for C_{max} while the AUC is slightly underpredicted. The AFE for profile prediction is of 0.81. The exposure in the fed state is predicted to be lower than in the fasted state which is consistent with a high first-pass extraction which could be saturated in the fasted state. The AFE for fed state profile prediction is of 0.79. In both prandial states, the fraction absorbed is anticipated to be 100%, but the fraction escaping first-pass gut metabolism (Fg) decreases from 31% (single emptying phase) or 17% (double emptying phase) in the fasted state to 13% in the fed state. The use of a mechanistic first-pass gut extraction in the model can show the impact of gastric emptying on the amount of drug lost by first-pass extraction. In the case of nefazodone HCl, both partial and multiphasic gastric emptying in the fasted state, or slower emptying in the fed state when the drug is trapped in the stomach with food, can reduce the C_{max} and the exposure compared to rapid gastric emptying where higher drug concentrations in the lumen and the enterocytes saturate first-pass gut extraction.

Furosemide

The model input parameters for furosemide are provided in Table II. The simulation of 40 mg furosemide IV bolus is shown in supplementary material 5. The oral PK profile estimation with GastroPlus™ is provided in Fig. 4 for the fasted and fed state. Using a bottom-up approach for the fasted state with an effective jejunal permeability of 0.5 led to PK predictions overestimating the AUC. Optimization consisted of adjusting the permeability in GastroPlus™ along the GI tract compartments to represent the upper GI absorption window reported in the literature (28) using a middle-out approach based on the fasted state data. Figure 4 shows the simulated profiles for the fasted and predictions of fed states before and after optimization in GastroPlus™. Predicted AUC and C_{max} and their ratios to the fasted state are within the 0.8–1.25 interval for GastroPlus™. The AFE and AAFE for profile prediction in the fasted state are of 0.9 and 1.29 respectively. The AFE and AAFE for profile prediction in the fed state are of 1.36 and 1.49 respectively.

Table II. Furosemide Modeling Input Parameters for Simcyp® and GastroPlus™

Parameter	Simcyp®	GastroPlus™	Reference/rationale
Molecular weight	330.7		(44)
Compound nature	Crystalline		
pK_a	3.9 (A)		(45)
Log *P*	2.56		(46)
True density (g/mL)	1.63		(47),
Intrinsic solubility (μg/mL)	13		(45, 46, 48, 49)
FaSSIF-V2 solubility (mg/mL)	3.201		(49)
FeSSIF solubility (mg/mL)	0.684		(49)
log ($K_{m:w}$)	Neutral: 4.478; ionized: 1E-6	NA	
Solubilization ratio	NA	1.07E+4	Fitted from solubility data in GastroPlus™
F_u plasma (%)	2.32		(50)
B/P ratio	1.34		(51)
Particle size diameter (μm)	10		Default value for the IQ consortium work
Duodenum P_{eff} (10^-4 cm/s)	0.5	1.2 (post optimization)	(28) An absorption window in the duodenum is present for this drug and is fitted to oral fasted state data (middle-out approach)
Jejunum P_{eff} (10^-4 cm/s)	0.5	0.5	(27)
All other compartment P_{eff}	0.5	0.05 (post optimization)	(27)
Formulation type	40 mg immediate release tablet		
Model for dissolution	Diffusion layer model	Johnson, adjust for BS effect on solubility and diffusion	
DLM scalar	1	NA	Default approach from (10)
Model for distribution	Minimal PBPK model	3 compartmental	
V_{ss} user input (L/kg)	0.076	NA	
SAC K_{in}, SAC K_{out} (h^{-1})	1.6, 2.6	NA	
V_c (L/kg), k_{12} (h^{-1}), k_{21} (h^{-1}), k_{13} (h^{-1}), k_{31} (h^{-1})	NA	0.0707, 1.606, 2.616, 0.239, 0.0588	Fitted to IV data of ref. (25)
IV clearance (L/h/kg)	0.139	0.133	From IV data (25) (for GastroPlus, 75% of the total clearance is attributed to the kidneys (24) $CL_R = 0.09975$ L/h/kg and $CL_H = 0.03325$ L/h/kg)

NA not applicable, *DLM* diffusion layer model, *PBPK* physiologically based pharmacokinetic, *B/P* blood to plasma, F_u fraction unbound, *FaSSIF* fasted state simulated intestinal fluid, *FeSSIF* fed state simulated intestinal fluid, *BS* bile salt

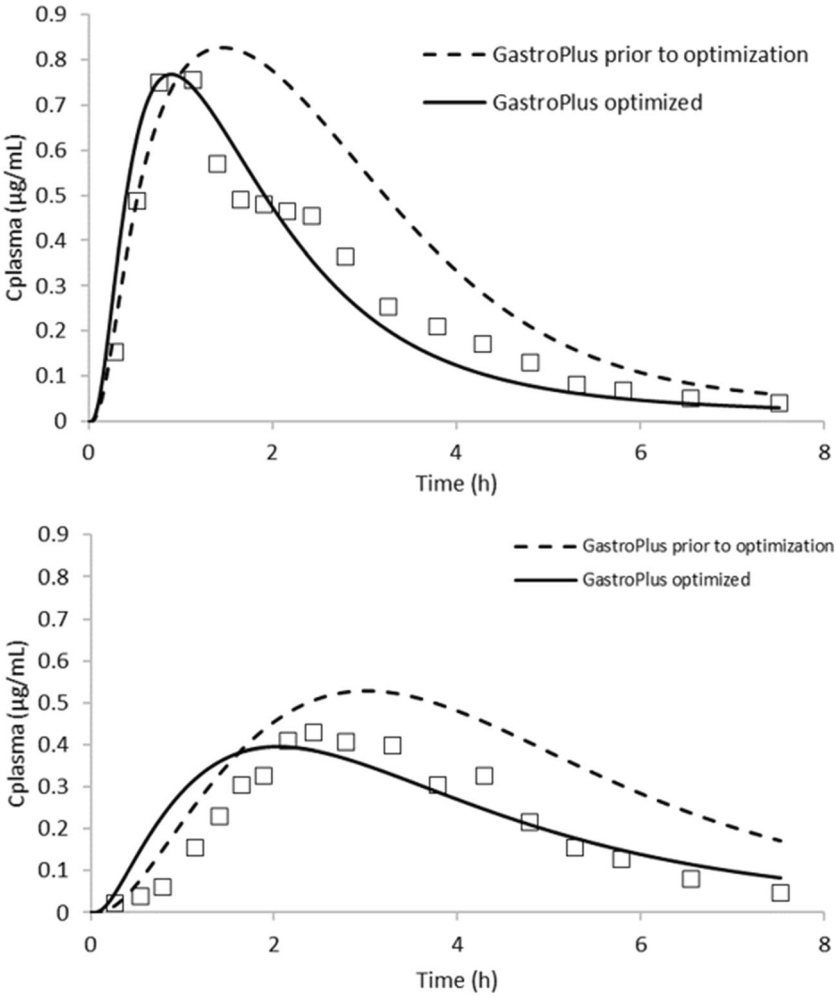

Fig. 4. Simulations of fasted (upper panel) and predictions of fed (lower panel) plasma concentration time profiles for 40 mg furosemide tablets with GastroPlus™. Symbols show observed data

Additional simulations were conducted with GastroPlus™ v9.7 where default fixed fluid volumes were reduced to 7.5% in the small intestine and 2% in the colon, or when the dynamic 100% Mudie model was used to predict fluid volumes in the GI tract (Fig. 5). In case of reduced fluid volumes in the GI tract for GastroPlus™, the fasted state simulation results between GastroPlus™ and Simcyp® are consistent and underestimate the absorption rate for furosemide.

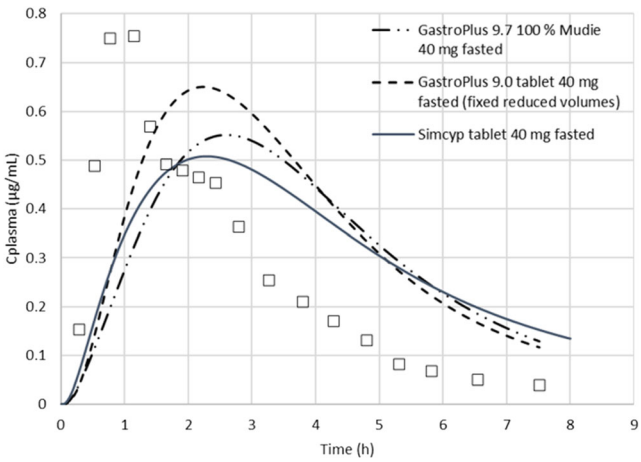

Fig. 5. Simulated plasma profiles for a 40 mg furosemide tablet dosed in the fasted state using default P_{eff} values for Simcyp® and GastroPlus™ but with fixed volumes in the GI tract for GastroPlus™ reduced to 7.5% in the small intestine and 2% in the colon or dynamic 100% Mudie model in GastroPlus™ V9.7. Symbols show observed data

Aprepitant

Since intrinsic solubility values reported in the literature varied by approximately 10-fold, oral PK simulations for 100 mg micronized and 125 mg nanosized suspensions in fasted state were compared using the low (0.7 µg/mL for micro and 1.3 µg/mL for nano) and high solubility values (7 µg/mL for both micro and nano) in Simcyp® which lead to PK parameters (i.e., AUC and C_{max}) which were under (0.39 and 0.25-fold) or overpredicted (2.2 and 1.63-fold) respectively (see supplementary material 4). When an average solubility value calculated from the low and high values reported in the literature was used for simulating fasted PK

Table III. Aprepitant Modeling Input Parameters for Simcyp® and GastroPlus™

Parameter	Simcyp®	GastroPlus™	Reference/rationale
Molecular weight	534.43		
Compound type	Weak base in the physiological pH range		
pK_a	9.15 (A); 2.45 (B)		See explanation in text
Log *P*	4.8		(32)
F_u plasma	0.05		(29)
B/P ratio	0.86		
Absorption model	ADAM	ACAT	
Fu enterocyte (%)	100		Default value
Human P_{eff} (10^-4 cm/s)	2.416 (same input for micronized)		This work: from MDCK $P_{app} = 13 \times 10^{-6}$ cm/s (recovery 65%) and propranolol reference at 15×10^{-6} cm/s
Formulation	IR solid formulation	IR tablet	
Dose	100 mg (micronized) 125 mg (nanosized)		
Precipitation	CSR: 10000 PRC(1/h): 0.0001 (for both micro and nano)	T_p = 9000 s for micronized and 900 s for nanosized	No impact of T_p on exposure
Volume in the GI tract	Default	7.5% in the small intestine and 2.5% in the colon	The use of default volumes in GastroPlus™ overestimated the exposure
Absorption scaling factors	NA	Log *D* model	The default ASF model in GastroPlus™ overestimated drug exposure
Intrinsic solubility (μg/mL)	3.8 (micronized) or 4.0 (nanosized) at pH 8.0		Average from reported values in references (32, 33)
FaSSIF-V2 solubility (μg/mL)	5.4 (micro), 13.6 (nano)		(33)
FeSSIF-V2 solubility (μg/mL)	92.4 (micro), 102 (nano)		
log ($K_{m:w}$)	Neutral (5.83) (micro) Neutral (5.61) (nano)	NA	Fitted using SIVA
Solubilization ratio	NA	1.07E+5 (micro) 3.15E+5 (nano)	Fitted using GastroPlus
Model for dissolution	DLM	*Z*-factor for micronized, Johnson for nanosized using nanofactor = 22.4	Fitted to dissolution data in FaSSIF and FeSSIF
Particle diameter (μm)	7 (micro), 0.12 (nano)	0.12 (nano)	(32, 33)
Z-factor (mL/mg/s)	NA	0.00569 (micro/fasted) 0.00575 (micro/fed)	Fitted to FaSSIF and FeSSIF dissolution data
DLM scalar	0.006 (fasted), 0.134 (fed) – micro; 0.001 (fasted), 2.384 (Fed) - nano	NA	Fitted to FaSSIF and FeSSIF dissolution data (see supplementary material 4)
Distribution model	Minimal PBPK	1 compartment model (V_c and IV clearance)	
V_{ss} user input (L/kg)	0.82	NA	(30)

Table III. (continued)

Parameter	Simcyp®	GastroPlus™	Reference/rationale
$K_{in}/K_{out}/V_{sac}$	0.16/0.18/0.13	NA	Optimized using parameter optimization module
V_c (L/kg)	NA	0.944	Single compartment used in GastroPlus
IV clearance (L/h/kg)	0.051	0.07234	Extensive metabolism (CYP3A4). No renal excretion, clearance extracted from IV data (30)

NA not applicable, *DLM* diffusion layer model, *PBPK* physiologically based pharmacokinetic, *B/P* blood to plasma, *ASF* absorption scaling factor, F_u fraction unbound, *FaSSIF* fasted state simulated intestinal fluid, *FeSSIF* fed state simulated intestinal fluid, *MDCK* Madin-Darby Canine Kidney, *CSR* critical supersaturation ratio, *PCR* precipitation rate constant, *SIVA* Simcyp in vitro analysis toolkit

profiles for micro and nano formulations, predictions of AUC and C_{max} values were within the pre-specified tolerance. The model input parameters for aprepitant are provided in Table III. The difference in IV clearance for aprepitant is related to different sources of measurement. As indicated in the "MATERIALS AND METHODS" section, Simcyp® model was built using the clearance measured using IV PK generated on top of an oral dose, whereas GastroPlus™ model was build using the PK data generated from IV dosing only. The Simcyp® model was used to predict the effect of food on PK of a 100 mg micronized aprepitant formulation and 125 mg nanoparticle suspension (Fig. 6). The predicted increase in aprepitant AUC and C_{max} in the presence of food is within 0.75–1.25-fold of the observed values (34). The model slightly overpredicted positive food effect but was within the pre-specified tolerance (33). Additional simulations with GastroPlus™, testing the impact of luminal volume and absorption scaling factors, are shown in supplementary material 4.

DISCUSSION

The tables summarizing predicted and measured PK parameters for the three drugs and four formulations of this work are found in supplementary material 6. This work presented a middle-out approach where initial mispredictions using a bottom-up approach for the fasted state were corrected during model verification. This work illustrates the need to sometimes inform models with *in vivo* data, for parameters which cannot be informed through *in vitro* data only, and more importantly, provides a framework to explore model mispredictions and optimize models in a scientific way (Figure S0.1). The hypotheses made during model verification and optimization should be verified *in vitro* or *in vivo* as much as possible. For these three examples, although the mechanism of food effect could be well captured by at least one software, the impact of GI fluid volume differences in both simulation platform default settings led to quantitative differences in the predictions. While the stomach fixed volumes in the fasted (approx. 50 mL) and fed (approx. 1000 mL) are similar for both GastroPlus™ and Simcyp®, the default volumes are very different for the small and large intestine (Fig. 7). In Simcyp® (or in GastroPlus™ V9.7), the fluid volumes are (or can be made) dynamic, reaching a peak value due to the water transfer from the previous compartment and water absorption by the gut membrane or transit to the next compartment. Neither model considers the volume of water present in the GI mucus as available for dissolution or solute dilution, which, depending on the type of formulation, may have an impact on the model performance and their comparison. A calculation of the mucus volume along each GI tract compartment is shown in supplementary material 7.

Default values for fixed fluid volume in GastroPlus™ are 2.7 times higher in the small intestine and 7.5 times higher in the colon compared to default values in Simcyp® over 1 h. When fixed volume occupation is reduced to 7.5% in the small intestine and 2% in the colon in GastroPlus™, the calculated luminal volumes are closer to that present in Simcyp® and reported in the literature (52, 53). When the dynamic 100% Mudie option is applied in GastroPlus™ v9.7, the 1-h average fluid volume values are lower than those

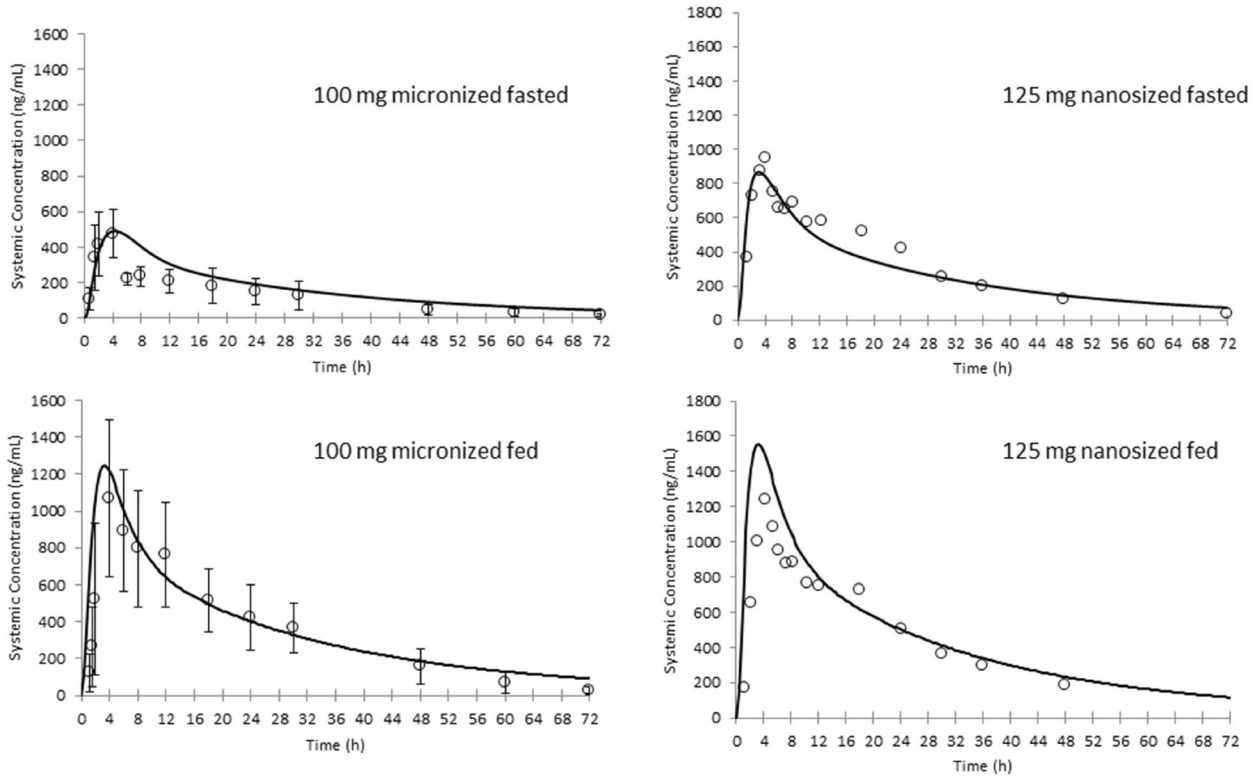

Fig. 6. Prediction of plasma concentration time profiles for fasted (upper panel) and fed state (lower panel) for 100 mg micronized formulations (left) and 125 mg nanosized formulations (right) of aprepitant using Simcyp®. Symbols show observed data ± 1SD

reported in the literature for the small intestine and colon. The duodenal volumes in GastroPlus™ are particularly low using the fixed volume reduction or 100% Mudie option over 1 h which could have an impact on the prediction of drug precipitation.

Nefazodone is an example of a drug where neither permeability, solubility, nor dissolution is limiting absorption. The scaling of metabolism mediated by CYP3A4 from the kinetic parameters measured in human liver microsomes was successful to predict the *in vivo* liver clearance in both software platforms (supplementary material 5). For nefazodone, the prediction of food effect based on AUC using GastroPlus™ was close to the population data (19) and to the data reported in the drug FDA label (18), i.e., a reduction of 20% exposure in the fed state. The main mechanism for the negative effect of food is a higher intestinal first-pass extraction in the fed state and this was well predicted by GastroPlus™. For compounds subject to a large first-pass extraction, and when the enterocyte free drug concentration range covers the $K_{m,u}$ of the gut enzyme isoforms, the gastric emptying pattern could be a key determinant of the exposure. One refinement for PBPK models in the future would be to calculate partial emptying or gastric residence in a more mechanistic way, through for example, a calculation of density, swelling, and disintegration

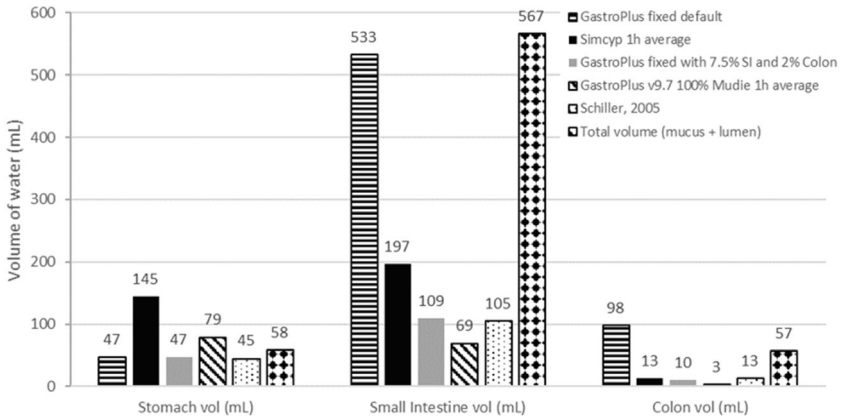

Fig. 7. Luminal volumes in the fasted stomach, small intestine, and colon for GastroPlus™ (fixed default, fixed reduced, and 1-h average dynamic 100% Mudie model in v9.7) and for Simcyp® (1 h average) compared to luminal volumes reported by Schiller and total luminal and mucus volumes

of the dosage form, use of the dosage form, aggregates, and individual particles' wettability and density to predict spatial segregation in the fasted and fed stomach phases, together with a more relevant description fluid velocities in relation to the prandial states and gastric emptying patterns. Although the same input parameters were used for Simcyp® for nefazodone HCl, and similar absorption profiles were predicted, the intestinal first-pass extraction was predicted to go down with food with this software. In both simulation tools, the free drug concentration in the lumen and enterocytes was lower in the fed state compared to the fasted state, consistent with drug dilution in the higher chyme volume in the fed state. GastroPlus™ predicted saturation of first-pass intestinal extraction in the fasted state, since the enterocyte concentrations were about 10-fold higher than the $K_{m,u}$ for CYP3A4. However, in Simcyp, the fasted concentration in the enterocytes was of the same order or lower than the CYP3A4 $K_{m,u}$, and hence there was no saturation of first-pass intestinal extraction in fasted or fed states. This observation can be explained by a predicted higher drug fraction absorbed in the upper part of the GI tract by GastroPlus™ and lower volumes for the enterocytes in GastroPlus™ compared to Simcyp® (supplementary material 3).

For furosemide, the adjustment of effective permeability along the GI tract based on fasted data for this drug (permeability was reduced from the duodenum to the colon) is qualitatively aligned with PgP expression level in the PBPK platform (expression goes up from the duodenum to the colon). Although the negative effect of food on C_{max} and $AUC_{0\text{-}t}$ is correctly predicted by GastroPlus™, using calculated bioavailability for both prandial states, a reduction of 3% exposure is predicted for furosemide in the presence of food (8% when using the more mechanistic P-gp model shown in supplementary material 2), which is smaller than the 18% reduction in bioavailability observed in the presence of food (25). Other phenomena could explain, for a solid dosage form, a reduction in exposure in the presence of food, such as a slower dissolution rate in the viscous environment of the chyme reported for similar compounds in the fed state (54). It seems that for both software platforms, the volume of fluid in the GI tract compartments plays a role in limiting the absorption rate in the fasted state for furosemide due to the low solubility. With default fluid volumes in the GI tract in GastroPlus™, the absorption rate is well estimated when permeability values are optimized to account for the drug absorption window (Fig. 4). However, when luminal volumes are reduced to make them more physiologically relevant, the absorption rate for furosemide is underpredicted by this software but moves closer to predictions obtained with Simcyp® (Fig. 5). The reason behind why default GI fluid volumes work better for GastroPlus™ could be a rapid diffusion of furosemide in the volume of water present in the mucus, as discussed below. Indeed, the total physiological fluid volume (lumen + mucus) is close to default fluid volumes for the small intestine in GastroPlus™ (Fig. 7). Furosemide is a small size drug and will be fully ionized with a negative charge at the mucus pH of 6.5. Since mucus itself is negatively charged (55), no significant barrier to diffusion is anticipated for this drug.

For micronized aprepitant, the magnitude of positive food effect predicted by Simcyp® is in agreement with the clinical data. The increase in exposure is due to enhanced dissolution, followed by rapid and complete absorption predicted by the software in fed state. For nanosized formulation in fasted state, the observed increase in oral exposure compared to the micronized aprepitant in fasted state was well predicted by Simcyp® due to higher amount of dissolved drug in the duodenum and jejunum. Prediction of exposure to nanosized or micronized aprepitant in the fasted using GastroPlus™ was comparable to those obtained in Simcyp® only when the fluid volume in the GI tract was reduced to 7.5% in the small intestine and 2.5% in the colon or when the dynamic 100% Mudie physiology was used (supplementary material 4). Aprepitant will be neutral at the mucus pH and since it is very lipophilic, the mucus diffusion could be slower than for furosemide. Nefazodone free base has similar physicochemical properties compared to aprepitant, but the hydrochloride salt form would be expected to confer micro-environmental charges to the drug particles during dissolution at intestinal pH, which could enhance the polar interactions with the mucus.

Despite intestinal mucus being mostly composed of water, drugs do not diffuse in the mucus with identical diffusion coefficients as those measured in water or with a given ratio based on size (56). This can be explained by a complex mucus composition comprising almost a third of lipids based on dry weight (57, 58). In addition, a monolayer of phospholipids protects the mucus interface with the lumen (59). For drug particles, mucus penetration is related not only to size but also to the surface properties and charge of these particles (60–62). The ionization of drug particles at different pH could also contribute to changing these surface properties (63) and favor polar interactions with the negatively charged mucus (64). Incorporating mucus compartments to the PBPK models, and predicting drug diffusion through its layer, as well as mucus secretion rate and erosion in the lumen, would bring the advantage to differentiate drugs, which dissolution is limited by the luminal volume (when diffusion in the mucus is slower than drug dissolution or transit or mucus secretion rate), from drugs which can access the entire fluid volume made from the lumen fluid and mucus fluid. In addition, for solid particles sufficiently small and with the adequate surface properties, accessing the mucus could prolong the GI transit time and allow to dissolve closer to the absorptive surface. As shown in Fig. 7, this adjustment is not trivial and would be of great importance for BCS class 2 and 4 drugs.

CONCLUSIONS

The three examples presented in this paper show how middle-out modeling approaches can be used to predict the magnitude and direction of food effects provided the model is verified on fasted state PK data (Figure S0.1). For nefazodone, a mechanistic clearance for the gut and liver was introduced. For furosemide, an absorption window was introduced and for aprepitant, the biorelevant solubility was determined from multiple solubility measurements. In all cases, these adjustments were supported by literature data and sensitivity assessment on the factors limiting absorption.

This modeling exercise has also shown how sensitive the model results are to assumptions or model options around GI

luminal fluid volume available for dissolution or diffusion. A hybrid approach not only considering low volumes in the GI lumen (similar to those observed in humans by MRI) but also accounting for solute dilution or nanoparticulate dissolution in the fluid volume present in the mucus is a recommended approach for PBPK models, together with mechanistic prediction of particle and drug dissolution and diffusion in mucus. This could provide for a better estimate of the *in vivo* dissolution for drug formulations which can access this mucus volume, and those that are confined to the lumen. This approach would also better estimate the local drug concentrations at the absorptive surface and in the enterocytes to manage mechanistic models for permeation or first-pass gut extraction. It is time to improve the GI tract compartmental models to account for lost volumes!

ACKNOWLEDGMENTS

The authors would like to thank Vasiliki Paraskevopoulou, Rikesh Dattani, and Zhizhou Fang for the measurements done on nefazodone HCl.

COMPLIANCE WITH ETHICAL STANDARDS

Conflict of Interest The authors declare that they have no conflict of interest.

SUPPLEMENTARY INFORMATION

The online version contains supplementary material available at https://doi.org/10.1208/s12248-020-00548-8.

REFERENCES

1. Fleisher D, Li C, Zhou Y, Pao L-H, Karim A. Drug, meal and formulation interactions influencing drug absorption after oral administration: clinical implications. Clin Pharmacokinet. 2012;36:233–54.
2. O'Shea JP, Holm R, O'Driscoll CM, Griffin BT. Food for thought: formulating away the food effect-a PEARRL review. J Pharm Pharmacol. 2019;71:510–35.
3. FDA, Assessing the effects of food on drugs in INDs and NDAs—clinical pharmacology considerations guidance for industry (2019 https://www.fda.gov/media/121313/download).
4. EMA, C. f. M. P. f. H. Use, Ed. (2012).
5. Koziolek M, Alcaro S, Augustijns P, Basit AW, Grimm M, Hens B, et al. The mechanisms of pharmacokinetic food-drug interactions-a perspective from the UNGAP group. Eur JPharm Sci. 2019;134:31–59.
6. Pentafragka C, Symillides M, McAllister M, Dressman J, Vertzoni M, Reppas C. The impact of food intake on the luminal environment and performance of oral drug products with a view to *in vitro* and in silico simulations: a PEARRL review. J Pharm Pharmacol. 2019;71:557–80.
7. Emami Riedmaier A, Lindley DJ, Hall JA, Castleberry S, Slade RT, Stuart P, et al. Mechanistic physiologically based pharmacokinetic modeling of the dissolution and food effect of a biopharmaceutics classification system IV compound—the Venetoclax story. J Pharm Sci. 2018;107:495–502.
8. Tistaert C, Heimbach T, Xia B, Parrott N, Samant TS, Kesisoglou F. Food effect projections via physiologically based pharmacokinetic modeling: predictive case studies. J Pharm Sci. 2019;108:592–602.
9. Li M, Zhao P, Pan Y, Wagner C. Predictive performance of physiologically based pharmacokinetic models for the effect of food on oral drug absorption: current status. CPT Pharmacometrics Syst Pharmacol. 2017;7:82–9.
10. Emami Riedmaier A, et al. Use of PBPK modeling for predicting drug-food interactions: an industry perspective. AAPS J. 2020;22:1–15.
11. Tsamandouras N, Rostami-Hodjegan A, Aarons L. Combining the 'bottom up' and 'top down' approaches in pharmacokinetic modelling: fitting PBPK models to observed clinical data. Br J Clin Pharmacol. 2013;79:48–55.
12. Serajuddin ATM, Jarowski CI. Effect of diffusion layer pH and solubility on the dissolution rate of pharmaceutical bases and their hydrochloride salts I: phenazopyridine. J Pharm Sci. 1985;74:142–7.
13. Pepin XJH, et al. Bridging *in vitro* dissolution and *in vivo* exposure for acalabrutinib. Part II. A mechanistic PBPK model for IR formulation comparison, proton pump inhibitor drug interactions, and administration with acidic juices. Eur J Pharm Biopharm. 2019;142:435–48.
14. Barbhaiya RH, Dandekar KA, Greene DS. Pharmacokinetics, absolute bioavailability, and disposition of [14C]nefazodone in humans. Drug Metab Dispos. 1996;24:91–5.
15. Barbhaiya RH, Marathe PH, Greene DS, Mayol RF, Shukla UA, Gammans RR, et al. Safety, tolerance, and preliminary pharmacokinetics of nefazodone after administration of single and multiple oral doses to healthy adult male volunteers: a double-blind, Phase I Study. J Clin Pharm. 1995;35:974–84.
16. Barbhaiya RH, Shukla UA, Chaikin P, Greene DS, Marathe PH. Nefazodone pharmacokinetics: assessment of nonlinearity, intra-subject variability and time to attain steady-state plasma concentrations after dose escalation and de-escalation. Eur J Clin Pharmacol. 1996;50:101–7.
17. Greene DS, Barbhaiya RH. Clinical pharmacokinetics of nefazodone. Clin Pharmacokinet. 1997;33:260–75.
18. FDA. (2001).
19. Dockens RC, Greene DS, Barbhaiya RH. The lack effect of food on the bioavailability of nefazodone tablets. Biopharm Drug Dispos. 1996;17:135–43.
20. Rotzinger S. Human CYP3A4 and the metabolism of nefazodone and hydroxynefazodone by human liver microsomes and heterologously expressed enzymes. Eur Neuropsychopharmacol. 2002;12:91–100.
21. Austin RP. The influence of nonspecific microsomal binding on apparent intrinsic clearance, and its prediction from physicochemical properties. Drug Metab Dispos. 2002;30:1497–503.
22. Benet LZ. Pharmacokinetics/pharmacodynamics of furosemide in man: a review. J Pharmacokinet Biopharm. 1979;7:1–27.
23. Smith DE, Lin ET, Benet LZ. Absorption and disposition of furosemide in healthy volunteers, measured with a metabolite-specific assay. Drug Metab Dispos. 1980;8:337–42.
24. Boles Ponto L, Schoenwald R. Furosemide (Frusemide) a pharmacokinetic/pharmacodynamic review (part I). Clin Pharmacokinet. 1990;18:381–408.
25. Hammarlund MM, Paalzow LK, Odlind B. Pharmacokinetics of furosemide in man after intravenous and oral administration. Application of moment analysis. Eur J Clin Pharm. 1984;26:197–207.
26. Collins PJ, Houghton LA, Read NW, Horowitz M, Chatterton BE, Heddle R, et al. Role of the proximal and distal stomach in mixed solid and liquid meal emptying. Gut. 1991;32:615–9.
27. Lennernäs H. Human *in vivo* regional intestinal permeability: importance for pharmaceutical drug development. Mol Pharm. 2014;11:12–23.
28. Lee WI, Yoon WH, Shin WG, Song IS, Lee MG. Pharmacokinetics and pharmacodynamics of furosemide after direct administration into the stomach or duodenum. Biopharm Drug Dispos. 1997;18:753–67.
29. Clinical pharmacology and biopharmaceutics review for Emend (NDA 21–549) (2003 https://www.accessdata.fda.gov/drugsatfda_docs/nda/2003/21-549_Emend_biopharmr.pdf).
30. Majumdar AK, Howard L, Goldberg MR, Hickey L, Constanzer M, Rothenberg PL, et al. Pharmacokinetics of

aprepitant after single and multiple oral doses in healthy volunteers. J Clin Pharmacol. 2006;46:291–300.
31. Wan H, Ulander J. High-throughput pKa screening and prediction amenable for ADME profiling. Expert Opin Drug Metab Toxicol. 2006;2:139–55.
32. Wu Y, Loper A, Landis E, Hettrick L, Novak L, Lynn K, et al. The role of biopharmaceutics in the development of a clinical nanoparticle formulation of MK-0869: a Beagle dog model predicts improved bioavailability and diminished food effect on absorption in human. Int J Pharm. 2004;285:135–46.
33. Shono Y, Jantratid E, Kesisoglou F, Reppas C, Dressman JB. Forecasting *in vivo* oral absorption and food effect of micronized and nanosized aprepitant formulations in humans. Eur J Pharm Biopharm. 2010;76:95–104.
34. Georgaka D, Butler J, Kesisoglou F, Reppas C, Vertzoni M. Evaluation of dissolution in the lower intestine and its impact on the absorption process of high dose low solubility drugs. Mol Pharm. 2017;14:4181–91.
35. Sanchez RI, Wang RW, Newton DJ, Bakhtiar R, Lu P, Chiu SHL, et al. Cytochrome P450 3A4 is the major enzyme involved in the metabolism of the substance P receptor antagonist aprepitant. Drug Metab Dispos. 2004;32:1287–92.
36. Li AC, Shou WZ, Mai TT, Jiang XY, Complete profiling and characterization of *in vitro* nefazodone metabolites using two different tandem mass spectrometric platforms. Rapid communications in mass spectrometry : RCM 21, 4001–4008 (2007).
37. Li M, Zhang H, Chen B, Wu Y, Guan L. Prediction of pKa values for neutral and basic drugs based on hybrid artificial intelligence methods. Sci Rep. 2018;8.
38. DrugBank. (2005), vol. 2019.
39. Poulin P, Theil FP. *A priori* prediction of tissue: plasma partition coefficients of drugs to facilitate the use of physiologically-based pharmacokinetic models in drug discovery. J Pharm Sci. 2000;89:16–35.
40. Davies NM, Takemoto JK, Brocks DR, Yáñez JA. Multiple peaking phenomena in pharmacokinetic disposition. Clin Pharmacokinet. 2012;49:351–77.
41. Pepin XJ, et al. Justification of drug product dissolution rate and drug substance particle size specifications based on absorption PBPK modeling for Lesinurad immediate release tablets. Mol Pharm. 2016;13:3256–69.
42. Andreas CJ, Pepin X, Markopoulos C, Vertzoni M, Reppas C, Dressman JB. Mechanistic investigation of the negative food effect of modified release zolpidem. Eur J Pharm Sci. 2017;102:284–98.
43. H. N. Joshi, N. Y. U. Bristol-Myers Squibb Company New York, Ed. (Jones, Alan John et al CARPMAELS & RANSFORD 43 Bloomsbury Square London, WC1A2RA (GB) AT BE CH DE DK ES FR GB GR IE IT LI LU MC NL PT SE 1995), chap. EP 0 710 653 B1.
44. Fioritto AF, Bhattachar SN, Wesley JA. Solubility measurement of polymorphic compounds via the pH-metric titration technique. Int J Pharm. 2007;330:105–13.
45. Rabbie SC, Flanagan T, Martin PD, Basit AW. Inter-subject variability in intestinal drug solubility. Int J Pharm. 2015;485:229–34.
46. Avdeef A, Berger CM, Brownell C. pH-metric solubility. 2: correlation between the acid-base titration and the saturation shake-flask solubility-pH methods. Pharmaceutical Research. 2000;17:85–9.
47. de Villiers MM, van der Watt JG, Lötter AP, Liebenberg W, Dekker TG. Correlation between physico-chemical properties and cohesive behavior of furosemide crystal modifications. Drug Dev Ind Pharm. 1995;21:1975–88.
48. Cvijic S, Parojcic J, Langguth P. Viscosity-mediated negative food effect on oral absorption of poorly-permeable drugs with an absorption window in the proximal intestine: *in vitro* experimental simulation and computational verification. Eur J Pharm Sci. 2014;61:40–53.
49. Takács-Novák K, Szőke V, Völgyi G, Horváth P, Ambrus R, Szabó-Révész P. Biorelevant solubility of poorly soluble drugs: rivaroxaban, furosemide, papaverine and niflumic acid. J Pharm Biomed Anal. 2013;83:279–85.
50. Viani A, Pacifici GM. Bilirubin displaces furosemide from serum protein: the effect is greater in newborn infants than adult subjects. Dev Pharmacol Ther. 1989;14:90–5.
51. Lee MG, Chen ML, Chiou WL. Pharmacokinetics of drugs in blood II. Unusual distribution and storage effect of furosemide. Research Communications in Chemical Pathology and Pharmacology. 1981;34:17–28.
52. Schiller C, et al. Intestinal fluid volumes and transit of dosage forms as assessed by magnetic resonance imaging. Aliment Pharmacol Ther. 2005;22:971–9.
53. Mudie DM, Murray K, Hoad CL, Pritchard SE, Garnett MC, Amidon GL, et al. Quantification of gastrointestinal liquid volumes and distribution following a 240 mL dose of water in the fasted state. Mol Pharm. 2014;11:3039–47.
54. Radwan A, Amidon GL, Langguth P. Mechanistic investigation of food effect on disintegration and dissolution of BCS class III compound solid formulations: the importance of viscosity: MECHANISM OF FOOD EFFECT FOR BCS CLASS III PRODUCT. Biopharm Drug Dispos. 2012;33:403–16.
55. Sigurdsson HH, Kirch J, Lehr CM. Mucus as a barrier to lipophilic drugs. Int J Pharm. 2013;453:56–64.
56. Khanvilkar K. Drug transfer through mucus. Adv Drug Deliv Rev. 2001;48:173–93.
57. Larhed AW, Artursson P, Bjork E. The influence of intestinal mucus components on the diffusion of drugs. Pharm Res. 1998;15:66–71.
58. Lichtenberger LM. The hydrophobic barrier properties of gastrointestinal mucus. Annu Rev Physiol. 1995;57:565–83.
59. Ehehalt R, Braun A, Karner M, Füllekrug J, Stremmel W. Phosphatidylcholine as a constituent in the colonic mucosal barrier-physiological and clinical relevance. Biochim Biophys Acta. 2010;1801:983–93.
60. Swavola JC, Edwards TD, Bevan MA. Direct measurement of macromolecule-coated colloid-mucus interactions. Langmuir : the ACS journal of surfaces and colloids. 2015;31:9076–85.
61. Lai SK, Wang YY, Hanes J. Mucus-penetrating nanoparticles for drug and gene delivery to mucosal tissues. Adv Drug Deliv Rev. 2009;61:158–71.
62. Yildiz HM, McKelvey CA, Marsac PJ, Carrier RL. Size selectivity of intestinal mucus to diffusing particulates is dependent on surface chemistry and exposure to lipids. J Drug Target. 2015;23:768–74.
63. Pepin X, Blanchon S, Couarraze G. Powder dynamic contact angle data in the pharmaceutical industry. Pharm Sci Technolo Today. 1999;2:111–8.
64. Boegh M, Nielsen HM. Mucus as a barrier to drug delivery–understanding and mimicking the barrier properties. Basic & Clinical Pharmacology & Toxicology. 2015;116:179–86.

Publisher's Note Springer Nature remains neutral with regard to jurisdictional claims in published maps and institutional affiliations.